SORPTION AND TRANSPORT OF SPECIES IN SILICALITE STUDY OF BINARY SYSTEMS CONTAINING IODINE*

Vladimir MASARIK[a], Pavel NOVAK[a], Arlette ZIKANOVA[a], Jan KORNATOWSKI[b], Jaroslav MAIXNER[c] and Milan KOCIRIK[a]

[a] *J. Heyrovsky Institute of Physical Chemistry, Academy of Sciences of the Czech Republic, 182 23 Prague 8, Czech Republic; e-mail: kocirik@jh-inst.cas.cz*

[b] *Institute of Technical Chemistry and Heterogeneous Catalysis, Technical University of Rheinland-Westfalen, D-52074 Aachen, Germany, and Faculty of Chemistry, N. Copernicus University, PL-87-100 Torun, Poland; e-mail: kornatowski@rwth-aachen.de*

[c] *Prague Department of Institute of Chemical Technology, 166 28 Prague 6, Czech Republic; e-mail: maixnerj@vscht.cz*

Received October 23, 1996
Accepted November 11, 1997

Sorption of iodine from both the vapour phase and iodine solutions in organic solvents on large Silicalite-1 crystals was investigated. The single component sorption of iodine and sorption from binary mixtures under co-diffusion conditions led to a uniform colouring of the crystals. Under counter-diffusion conditions with crystals saturated initially with vapour of a selected solvent, the sorption kinetics of iodine was 2 or 3 orders of magnitude slower as compared with the corresponding co-diffusion experiment. Colouring of crystals was always, at least in its initial stage, non-uniform with visualized pyramids at crystal basal planes. This finding together with the nature of outer and inner crystal morphology suggests that our Silicalite-1 crystals are 90°-intergrowths which have only pore mouth openings of sinusoidal channels in the crystal surface. The process of crystal colouring under counter-diffusion conditions seems to proceed *via* diffusion along the boundaries of crystal sections.
Key words: Silicalite-1; Iodine; Binary sorption; Diffusion; Zeolites.

Since the beginning of the eighties, the investigation of mass transport in zeolites of MFI structure type has become of interest mainly due to their importance in shape selective catalysis. This interest has still been rising in the last decade due to efforts with the preparation of the zeolite-based molecular sieve membranes. For this reason, the intracrystalline mass transport and molecule mobility in zeolite channels have extensively been investigated using various techniques like NMR (refs[1–4]), FTIR (refs[5–7]),

* Presented at the *Symposium on Diffusion in Zeolites and Other Microporous Materials at the 12th CHISA '96 Congress, Prague, August 25–30, 1996.*

classical sorption methods[8,9], frequency response method[10,11], flow techniques[12,13] and permeation of gases through the crystals[14,15].

An approach promising to bring a progress in understanding the sorption kinetics and intracrystalline mass transport consisted in observations of large and well-defined crystals. It gave a possibility to investigate more complex processes like diffusional anisotropy[16], combined intracrystalline diffusion and transport through a mass transport resistance at crystal surface[17], combined intracrystalline diffusion and immobilization processes in crystal interior[8,13], *etc*.

One aspect which has not been analysed sufficiently in relation to intracrystalline mass transport is, to our opinion, the morphology of crystals of the MFI structure type. It is so because crystals grown from solutions are generally composed of several crystal sections which may differ in crystallographic order separated from each other by interfaces of distinct physical properties. Figure 1 shows a typical habitus of crystals with the MFI type structure together with crystal size parameters L_a, L_b, L_c.

Two kinds of crystals with the MFI type structure are considered below which differ from each other in arrangement of crystal sections:

a) Crystals of flat form with edges $L_a \neq L_b \neq L_c$ composed at least of 3 or more likely 6 wedge shaped parts (sections) which have the same crystallographic order are usually referred to as monocrystals because this arrangement cannot be distinguished from a true monocrystal by X-rays. A model of such a crystal which shows the individual crystal sections has been given by Caro *et al.*[16] and by Geus *et al.*[18] and is presented in Fig. 2. The authors of the above model assumed a hindrance for the mass transfer across the boundary of the sections[18].

b) Another form of the crystals which may look apparently as monocrystals is a so-called 90°-intergrowth. These crystals are regular in form with $L_a = L_b \neq L_c$. In most cases such crystals are also composed of 3 or 6 crystals (sections) as in the former case but here the internal order of particular parts is turned by 90°, *i.e.* ***a*** and ***b*** axes and also directions of the channels are changed. A model showing the arrangement of individual crystal sections in 90°-intergrowth has been given by Weidenthaler *et al.*[19] (*cf.* Fig. 3). In Fig. 3, two pyramids of individuum I with a specified orientation are embedded into two pyramidal cavities of prismatic body (individuum II). The crystallographic axes ***a***

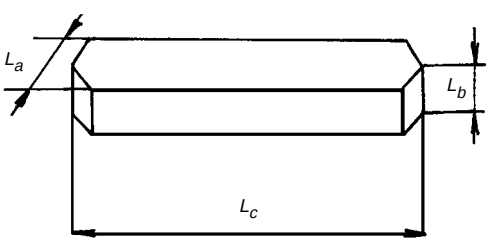

FIG. 1
Habitus of Silicalite-1 crystal together with its characteristic dimension parameters L_a, L_b and L_c

and ***b*** of individuum II are rotated by 90° about the axis ***c***. The 90°-intergrowths for the MFI structure type has also been reported by other authors[16,20–22].

Hypothetical properties of the above two kinds of the crystals from the point of view of mass transport are summarized below, based on a schematic representation of the crystal and the channel system cross-section within a cut perpendicular to axis ***c*** shown in Fig. 4. Crystallographic axis ***c*** is perpendicular to the plane of drawing, crystallographic axes ***a*** and ***b*** are oriented along sinusoidal channels and straight channels, respectively, and therefore the orientation of these axes in plane of drawing is given by the orientation of the respective crystal section. Note that only those channel systems are presented in Fig. 4 which have the respective pore mouth openings in the crystal surface. For the sake of simplicity we did not present in Fig. 4c the corresponding portion of straight channels (oriented along ***b***) which have their pore mouth openings in

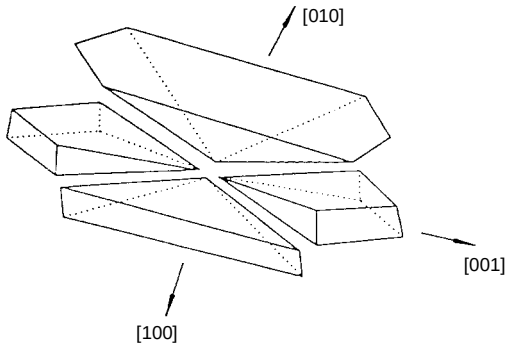

FIG. 2
MFI crystal sections (for clarity of both [100] and [010] sections, only one is shown). Reprinted with permission of the publisher from ref.[18]. Copyright 1994 by Elsevier Science Inc.

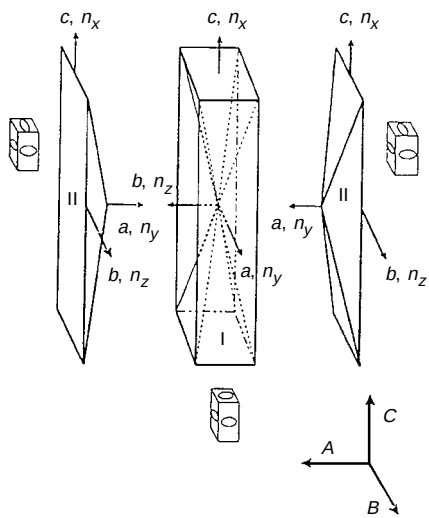

FIG. 3
Model of the ZSM-5 and Silicalite intergrowth. The orientation of the optical indicatrix for orientations *A*, *B*, and *C* is given together with the assignments of the crystal axes for the two individuals. Reprinted with permission of the publisher from ref.[19]. Copyright 1994 by American Chemical Society.

narrow stripes on the surface forming the steps along the long crystal edges (parallel to crystallographic axis ***c***).

In an ideal case when no barriers for the mass transport across the interfaces between sections would exist, the sorption kinetics would exhibit the same behaviour for the real arrangement of crystal sections described above (*cf.* Fig. 4a) and the true monocrystals. The authors of the monocrystal model postulated, however, hindrances for mass transport across the interface of crystal sections. Therefore, one would expect a difference in non-stationary sorption kinetics between the arrangement of crystal sections described in Figs 2 and 4a and the true monocrystals. This difference would be due to a hindered diffusion into [001] sections. In permeation experiments, the difference should be ever more dramatically dependent on the real resistance to mass transport across the interface surfaces.

The 90°-intergrowth materials reveal a similar situation with respect to the resistance to mass transport across the present interfaces as the monocrystals. The principal difference consists in the fact that mostly or even only sinusoidal channels are accessible

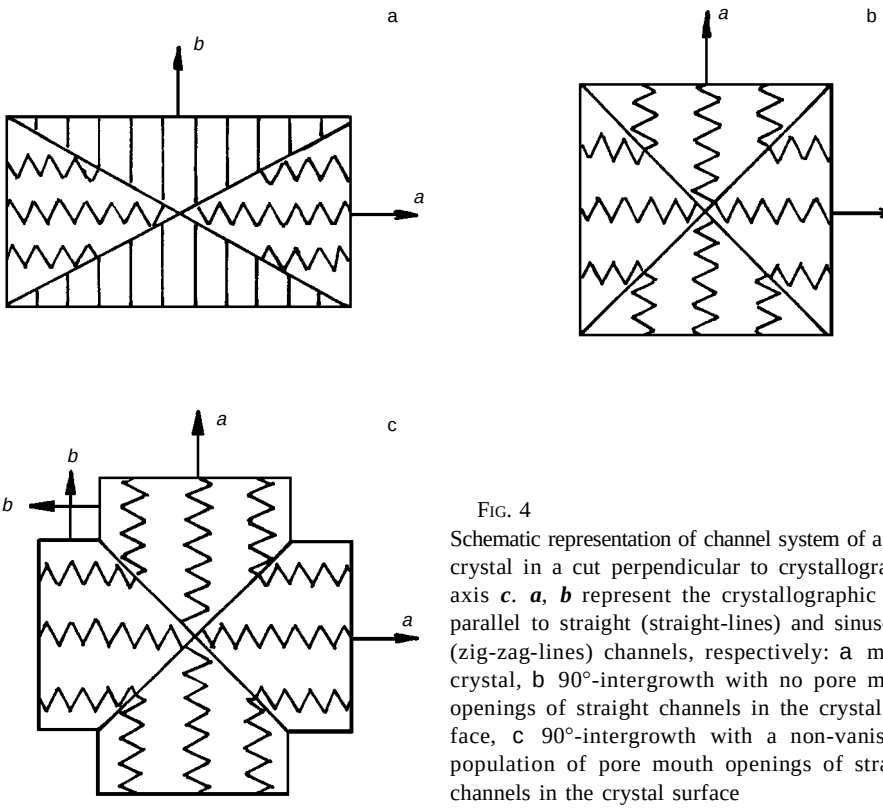

FIG. 4
Schematic representation of channel system of a MFI crystal in a cut perpendicular to crystallographic axis ***c***. ***a***, ***b*** represent the crystallographic axes parallel to straight (straight-lines) and sinusoidal (zig-zag-lines) channels, respectively: a monocrystal, b 90°-intergrowth with no pore mouth openings of straight channels in the crystal surface, c 90°-intergrowth with a non-vanishing population of pore mouth openings of straight channels in the crystal surface

from the crystal surface. It can be seen from Fig. 4b. In dependence on the particular form of the intergrowth which can be reflected also in outer crystal morphology, a non-vanishing population of pore mouth openings of straight channels may occasionally occur in the crystal surface (*cf.* Fig. 4c).

Such a diversity of crystal forms opens a field for speculations when interpreting the sorption kinetics. Thus, a need arises in a direct observation of a space distribution of species sorbed in zeolite crystals. There are two classical studies on the application of polarisation microscopy to a direct observation of diffusion in the crystals of natural zeolites by Tiselius[23,24]. In the seventies, the interference microscopy has been introduced by Kärger and co-workers to investigate the intracrystalline diffusion of water in A zeolites[25].

Recently we have developed in our laboratory a combination of transmission light microscopy with colouring techniques using iodine to visualize sorption and mass transport of sorbed species in the large zeolitic crystals. In the present paper, we report on that technique and focuse our attention on sorption of pure iodine and its binary mixtures with light aromatics in the Silicalite-1 crystals as well as on the role of the crystal morphology in these phenomena.

EXPERIMENTAL

Sorbed Species

Iodine (Lachema, p.a.), benzene (Fluka, puriss. p.a.), toluene (Spolana Neratovice, for UV analysis), *p*-xylene (Fluka puriss., standard for GC).

Sorbent

The Silicalite-1 crystals of uniform size were grown by reacting silica sol (Czech industrial product Tosil, Tonaso Nešt mice), tetrapropylammonium bromide (TPABr, Fluka, purum) used as a structure directing species (template) and sodium bicarbonate (Solvay France s. A., qualite 0–13). The reacting gel of the composition 90 SiO_2 : 12 Na_2O : 2 000 H_2O : 5 TPABr was heated in teflon-lined stainless steel autoclaves at 457 K for 190 h without agitation. Then the heating of autoclaves was stopped and after slow air-cooling to the ambient temperature, the crystals were filtered, washed and dried as usual. As-synthesized crystals were calcined in an O_2 stream using the following temperature program: heating up at 10 K h^{-1} to 393 K, keeping at 393 K for 12 h, heating up at 30 K h^{-1} to 823 K, then keeping at 823 K for 12 h. After cooling to the ambient temperature, the crystals were washed repeatedly with 1 M NH_4NO_3 solution and dried. The second calcination followed at the same conditions as the first one. After the above series of operations, the carbon content in the solid phase is found to be below the detection limit of elemental analysis, and it is assumed that all the molecules of organic template (TPABr) are removed from the zeolite channels on burning off. Such samples are referred to as template-free ones.

The crystals were characterized by SEM (Scanning Electron Microscopy) method which gives the information on the external morphology of the crystals (*cf.* Fig. 5). The crystals prepared using the above preparation method (it is referred to as the Hayhurst and Kornatowski[26] procedures) were mostly isolated crystals uniform in size and shape. The average crystal dimensions are: $L_a \approx 43$ μm,

$L_b \approx 43$ μm, $L_c \approx 217$ μm. Only a minor fraction of the crystallization product was represented by aggregates (interpenetration twins) of two or more crystals (X shaped aggregates or rosettes). As it can be seen from Fig. 5, the crystals are square-shaped in the cross-section ($L_a \approx L_b$).

The peculiarities of crystal interior were revealed using techniques of light microscopy (shearing technique) which visualizes the boundaries between individual crystal sections.

For Silicalite-1 crystals from our synthesis, the single crystal XRD (X-Ray Diffraction) did not provide any direct evidence that the crystals are 90°-intergrowth because the splitting of reflexion [101] which was observed for the cases when a small amount of Al was present (with Si/Al ratio in crystalline product ≈ 140) could not be detected in the absence of Al. Nevertheless, we concluded on the basis of SEM and light microscopy and on the basis of the development of colouring patterns described below that our Silicalite-1 crystals are 90°-intergrowths.

Light Microscopy

For optical observations of sorption, transmission light microscopy has been used with a microscope Peraval Interphako (Carl Zeiss, Jena). To examine the sorbent loaded with volatile species, a glass cell, consisting of intrinsic single covering glass, has been used which had the total thickness of about 2.5 mm (including the cover glass) and a cylindrical internal space (15 mm in diameter and 1.2 mm in depth).

All the optical observations were performed at the laboratory temperature of 298 K in the air and at the same fugacity of iodine in the fluid phase. Regardless of whether the sorption of iodine was performed from vapour or liquid phase, the fugacity of iodine was maintained to be equal to the saturated vapour pressure of iodine at 298 K. The effect of the presence of water preadsorbed on Silicalite-1 was tested and no perceptible influence was found. The following types of the experiments were performed.

Sorption of Iodine from Vapour Phase

Prior to the experiment beginning, the crystals were spread in a loose crystal monolayer on the bottom of the cell. At the same time the cell was in the air so that also crystal interior was filled with the air. The beginning of the experiment is defined by placing fine iodine particles into the cell. Thus, iodine particles act as a permanent source of iodine vapour maintaining the constant partial pressure of iodine at their surfaces. The sorption kinetics was monitored by taking colour photo-

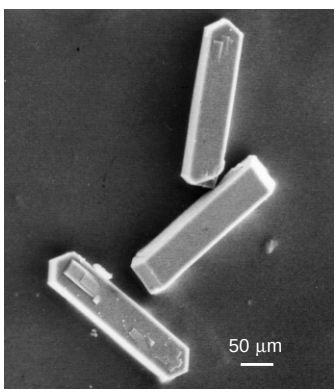

FIG. 5
SEM micrograph of Silicalite-1 crystals used in the present study

graphs of the crystals at different contact times τ_v (subscript v stands for iodine vapour) to evaluate uniformity of colouring process and to estimate a minimum contact time τ_v^∞ when a limiting (*i.e.*, maximum) intensity of crystal colouring was reached.

Sorption of Iodine from Solutions in Organic Solvents

The approach applied is based on the fact that for microporous solids there is no difference between the sorption of species from a solution and from the equilibrium vapour phase above this solution. The only constraint is that one cannot realize other situations than those corresponding to the vapour–liquid equilibrium at the temperature of sorption. The experiments from solutions were performed either under the co-diffusion or counter-diffusion conditions.

Co-diffusion experiments. In the co-diffusion experiments, an excess of a saturated solution of iodine in a chosen organic solvent was brought for a defined contact time τ_m (subscript m stands for saturated solution of iodine in an organic solvent) into contact with Silicalite-1 crystals, and then the liquid phase was quickly separated from the crystals under suction through a sintered glass filter in the bottom of the vessel. All this operation proceeded under agitation on a shaking apparatus. After the separation, the sample was immediately transferred into the cell for the optical observations.

Counter-diffusion experiments. In the counter-diffusion experiments, the crystals were brought into contact with the solvent first. The contact time τ_s (subscript s stands for organic solvent) was several days. Then the experiment followed the operations specified above for the co-diffusion experiment. The only difference was that in many cases the value of contact time τ_m^∞ necessary to reach the limiting colouring intensity or colouring pattern was 2 or even 3 orders of magnitude higher than that for the corresponding co-diffusion experiment.

RESULTS AND DISCUSSION

In the experiments with template-free samples and with no preadsorbed species, the sorption kinetics of iodine appeared to be limited by the external mass transport of iodine through a stagnant layer of air in the cell. When the source of iodine vapours was placed at the cell circumference, a colouring gradient over the sample was observed while the individual crystals exhibited a uniform colouring. The limiting colouring of the crystals was not attained within $\tau_v = 10$ min due to a large distance between source of iodine vapours and zeolite crystals. Figure 6 provides the evidence that the iodine transport is considerably facilitated compared with the previous arrangement when, at the experiment beginning, the iodine grains are scattered among the crystals. This picture was taken after contact time $\tau_v = 4$ min. There was no change in colouring intensity for the same configuration after $\tau_v = 1$ h. Thus, a direct observation with selected mutual configuration of crystals and iodine grains (the examined configuration is defined by white box in Fig. 6) enabled us to estimate a contact time τ_v^∞ to reach the maximum intensity of crystal colouring. The kinetics of the colouring process was examined repeatedly for different zeolite crystals located in between two large iodine particles. In all the cases a configuration of iodine and crystal grains was chosen within the field of scattered iodine particles and zeolite crystals with a distance of the crystal from each iodine particle to about 100 μm and the values of the contact time τ_v^∞ to reach the maximum intensity of crystal colouring ranged from 90 to 240 s.

The contribution of external diffusion of iodine through a stagnant air layer to the overall iodine sorption kinetics can be estimated using the following model which reflects the configuration described in the previous paragraph. A crystal of the edge lengths $L_a \approx L_b \approx 43$ μm approximated by an infinite plate of the thickness $2R = 43$ μm is assumed to be placed between two semiinfinite iodine blocks with surface parallel to the crystal surface and localized at the distance L from the crystal surface. Then, under the quasistationary state when a sorption equilibrium for iodine at crystal surface ruled by the Langmuir sorption isotherm is established instantaneously, one can write the following implicite equation for the relative molecular uptake γ (for the details of the mathematical model see Appendix):

$$(1 - \gamma)^{(1-\Theta)} = \exp(\gamma\Theta - u) \ , \quad 0 \le \gamma \le 1 \ . \tag{1}$$

The relative molecular uptake γ is defined in Symbols. For the sorbent free of sorbing species at the experiment beginning, γ can be expressed as

$$\gamma = \bar{a}/a_s \ , \quad 0 \le \gamma \le 1 \ . \tag{2}$$

Parameter Θ defined as

$$\Theta = a_s/a_\infty \ , \quad 0 \le \Theta \le 1 \tag{3}$$

denotes the loading of the crystals by iodine at its vapour concentration c_s. Here $\bar{a}$ denotes the adsorbed amount averaged over volume of the sorbent and a_s, a_∞ denote the equilibrium and the limiting adsorbed amounts of iodine, respectively. The parameter u which represents a dimensionless time parameter of colouring kinetics is defined by Eq. (*4*)

$$u = t \frac{D_{I_2N_2}}{RLS} \ . \tag{4}$$

In Eq. (*4*), $D_{I_2N_2} \approx 0.024$ cm^2 s^{-1} approximates the diffusion coefficient for the air–iodine mixture at ambient pressure (calculated by the method of Fuller, Schechttler and Giddings[27]), t denotes the time measured from the beginning of the colouring experiment, S represents the slope of the secant of sorption isotherm between the concentrations $c = 0$ and $c = c_s$. The minimum effect of external diffusion occurs for the limiting case of rectangular sorption isotherm (Θ = 1). In this case the differential equation of sorption kinetics has a singular point at $u = 1$, $\gamma = 1$ (*cf.* Eq. (*A14*) in Appendix) and the

uptake γ is accomplished at finite time ($u = 1$). Thus, $\gamma = u$ for $u \leq 1$, and $\gamma = 1$ for $u \geq 1$. Then it follows for $\gamma = 0.9$:

$$t_{0.9} = 0.9 \frac{RLS}{D_{I_2N_2}} \quad . \tag{5}$$

Based on our sorption measurements performed at 298 K, the limiting adsorbed amount of iodine in Silicalite-1 can be assesed $a_\infty \approx 3.44 \,.\, 10^{-3}$ mol cm^{-3}. Thus, for $c_s = 1.65 \,.\, 10^{-8}$ mol cm^{-3} (which corresponds to the saturated vapour pressure of iodine at the ambient temperature), the corresponding value of the slope S of sorption isotherm can be estimated at $S \approx 2.08 \,.\, 10^5$. Taking $R = 21.5$ μm, $L = 0.01$ cm, one obtains, on the basis of Eq. (*5*), the relation $t_{0.9} \approx 167$ s for the rectangular sorption isotherm. For the linear sorption isotherm, $\Theta \to 0$ and the numerical value of the coefficient in Eq. (*5*) becomes 2.3 instead of 0.9. Then the relation for $t_{0.9}$ changes to $t_{0.9} \approx 428$ s. One can conclude, by comparing these estimates for $t_{0.9}$ with those for τ_v^∞ obtained on the basis of iodine sorption from vapour phase ($\tau_v^\infty \in \langle 90\text{ s}, 240\text{ s}\rangle$), that under the conditions of a close contact of iodine with crystals, the sorption kinetics of iodine is most probably limited exclusively by external mass transport throughout the air layer.

Equations (*1*) and (*5*) give a criterion to estimate the contribution of external mass transport to the iodine sorption kinetics from the vapour phase for any particular configuration of zeolite–iodine particles selected on the photograph of the colouring process.

It should also be noted that the previous measurements[28] of self-diffusion of sorbed species in faujasite performed by NMR technique in the presence of permanent gases suggested that there was no influence of permanent gas on the self-diffusion coefficients for intracrystalline mass transport and, in our opinion, these results can be extended to Silicalite-1.

Sorption of Iodine from Liquid Phase: Co-Diffusion Experiments

In all the observations of this kind, the colouring of the crystals appeared to be uniform throughout the crystals. The maximum colouring intensity has been reached within several minutes, and it is assumed that also in this case the external diffusion affects strongly the sorption kinetics.

Sorption of Iodine from Liquid Phase: Counter-Diffusion Experiments

In this study, the diffusion of iodine against three aromatic molecules cylindrical in shape and essentially of the same value of critical diameter but different in molecule length is observed. The solvents selected are benzene, toluene and *p*-xylene.

In all these experiments, the space distribution of colouring of the crystals was, at least in its initial stage, non-uniform. It started to proceed from the basal planes of the crystals. Also the cracks in crystals were visualized being decorated with iodine.

System: Iodine–Benzene

For the iodine–benzene system, the pyramids are intensively coloured after a relatively short contact time τ_m = 30 min (*cf.* Fig. 7). After the contact time τ_m = 3 h, the remaining part of the intracrystalline space starts to be coloured and in 24 h the crystals seemed to be coloured uniformly. An observation of the last situation in polarized light (*cf.* Fig. 8) shows, however, that there are still less coloured places at both ends of crystals when observed from the lateral plane. It should also be noted that decoration of a crack in Fig. 7 is more diffuse as compared with that in all the other systems described below (*cf.* the diffuse line oriented along ***c*** axis on the central crystal in Fig. 7).

System: Iodine–Toluene

For the iodine–toluene system, the colouring of the crystals was much slower. It can be seen from Fig. 9, which shows the situation after the contact time τ_m = 6.5 h, and from Fig. 10 taken after the contact time τ_m = 140 h. Even after τ_m = 500 h, no colouring of the central part of the crystals was observed.

System: Iodine–p-Xylene

Diffusion of iodine against *p*-xylene proceeds in a similar way as toluene but the process of colouring of the pyramids was considerably slower compared with toluene, *i.e.*, the colouring intensity of pyramids after the contact time τ_m = 24 h was considerably lower than that for toluene after the contact time τ_m = 6.5 h. No perceptible effect of the magnitude of τ_s on the colouring process was found when changing the τ_s within the time interval 48 to 800 h. Thus, no change in packing of solvent molecules within zeolite channels occurs after τ_s = 48 h.

Hypothesis on the Nature of Colouring Process Under Counter-Diffusion Conditions

The above behaviour of all the three aromatics could be explained assuming that counter-diffusion of iodine against an aromatic molecule proceeds more easily in straight channels than in sinusoidal ones provided the Silicalite-1 crystals would be monocrystals (*cf.* Fig. 1). In such a case, the pyramids would be coloured with iodine in their bulk. The results of microscopy suggest, however, that our crystals are most likely 90°-intergrowths of the type shown in Figs 3 and 4b. Thus, most probably, the crystal surface has exclusively pore mouth openings of sinusoidal channels. Under

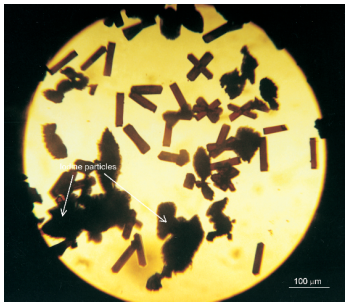

FIG. 6
Silicalite-1 crystals coloured after the contact with iodine from vapour phase, τ_v = 4 min

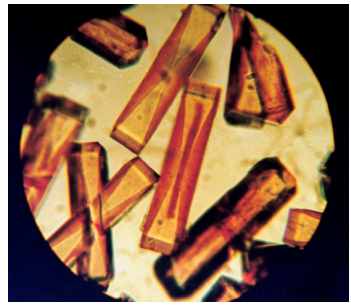

FIG. 7
Silicalite-1 crystals coloured after the contact with iodine from liquid under counter-diffusion conditions, solvent: benzene, τ_s = 48 h, τ_m = 30 min

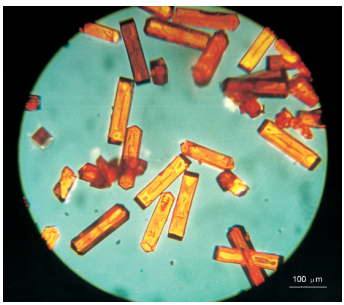

FIG. 8
Silicalite-1 crystals coloured after the contact with iodine from liquid under counter-diffusion conditions (observed in polarized light), solvent: benzene, τ_s = 48 h, τ_m = 24 h

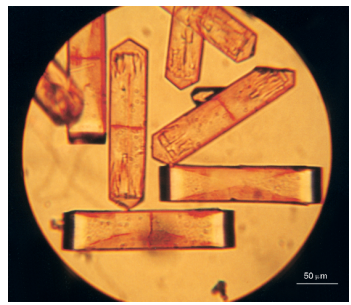

FIG. 9
Silicalite-1 crystals coloured after the contact with iodine from liquid under counter-diffusion conditions, solvent: toluene, τ_s = 24 h, τ_m = 6.5 h

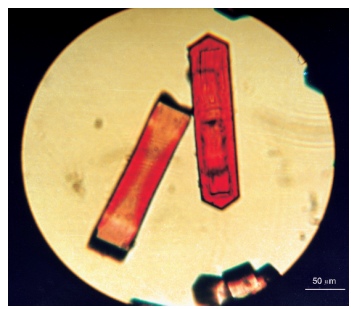

FIG. 10
Silicalite-1 crystals coloured after the contact with iodine from liquid under counter-diffusion conditions, solvent: toluene, τ_s = 24 h, τ_m = 140 h

these circumstances, the only plausible explanation is that the pyramids are not coloured in their bulk but the iodine particles start to penetrate along the interface of the pyramids in a way similar to diffusion along grain boundaries in metals[29]. From the interface, the iodine molecules penetrate in some depth of straight channels which visualizes the interface and makes an impression of bulk colouring of pyramids for the observation both from the basal and lateral sides of the crystals. Particularly, the results of observations of early stages of colouring process support this hypothesis. In many cases, we can see at the beginning only red lines located at the interface. Also it can be seen that the colouring of the interfaces starts from line sources at crystals edges (*cf.* a non-uniform colouring of pyramids and occurrence of red lines along the edges in Fig. 9).

There is a marked effect of molecule length both on the colouring of the crystals and on the decoration of cracks. For the iodine–toluene system, the decoration of cracks is significantly sharper compared with that for the iodine–benzene system (*cf.* Figs 7 and 9). At the moment we have no definite mechanistic explanation of this effect. The single component diffusion coefficients for intracrystalline diffusion of aromatics in MFI type zeolites do not differ significantly (*cf.*, *e.g.*, the data for the benzene–Silicalite-1 and *p*-xylene–Silicalite-1 systems in ref.[1]). Thus, the revealed drastic difference in behaviour of the above three systems may be due to some specific conditions in binary system at high coverage where the ability of aromatic molecules to reorientate may be of crucial importance.

CONCLUSIONS

The colouring of the template-free Silicalite-1 crystals is uniform and sorption kinetics of iodine from vapour phase is limited by external diffusion. The sorption of iodine from organic solvents on unloaded crystals leads to an uniform colouring of the crystals and sorption kinetics is most likely limited exclusively by external diffusion. Sorption rate of iodine from an organic solvent into crystals filled with this solvent at vapour pressure $p = p_s$ is about 2 or 3 orders or magnitude lower compared with the corresponding co-diffusion experiment. The colouring of the crystals in counter-diffusion experiments is, at least in the first stage of the process, non-uniform in crystal bulk, and pyramids at crystal basal planes are visualized. The visualization of the pyramids proceeds *via* diffusion of iodine along interface of crystal sections and the subsequent broadening of this trace. In the series benzene, toluene, *p*-xylene, the rate of colouring process decreases as the molecule length increases.

APPENDIX

Equation (*1*) has been presented above to estimate the effect of external diffusion of iodine through a stagnant air layer between iodine source and zeolite crystal on the overall sorption kinetics of iodine in the crystal. Below, Eq. (*1*) is derived.

Model Statement

1. The configuration of zeolite crystal and iodine source assumed is shown in Fig. 11. The zeolite crystal is of the shape of an infinite slab of the thickness $2R$ and iodine source is represented by two semiinfinite iodine blocks located at distance L from the crystal surface oriented in parallel with crystal surface. Parameter x represents the space coordinate measured from the plane of symmetry of the crystal and oriented along the outward normal of the surface.

2. The rate limiting step of the iodine sorption kinetics is the iodine diffusion throughout a stagnant air layer in the space between the iodine source and crystal surface, *i.e.*, possible effects of convection are neglected based on the geometry of the configuration. Thus, diffusion would be governed by the second Fick law with the corresponding binary diffusion coefficient which we approximate by the coefficient $D_{I_2N_2}$. The consequence of this assumption is that the iodine concentration is uniform throughout the crystal, and therefore the mean adsorbed amount $\bar{a}$ is equal to the local adsorbed amount everywhere in the crystal and also to the surface adsorbed amount a_R.

3. Prior to the experiment beginning, the gas phase and the crystal are free of iodine.

4. The sorption capacity of crystal volume unit with respect to iodine is 5 orders of magnitude higher compared with the amount of iodine accumulated in the unit volume of the gas phase. Thus, in a short time a quasistationary state is established in the gas phase.

5. At $x = R$, the adsorption equilibrium governed by the Langmuir adsorption isotherm is established instantaneously between slowly increasing concentration c_R and the adsorbed amount a_R in the crystal surface.

6. At $x = R + L$, the concentration c_s is established according to the vapour–solid equilibrium at iodine surface.

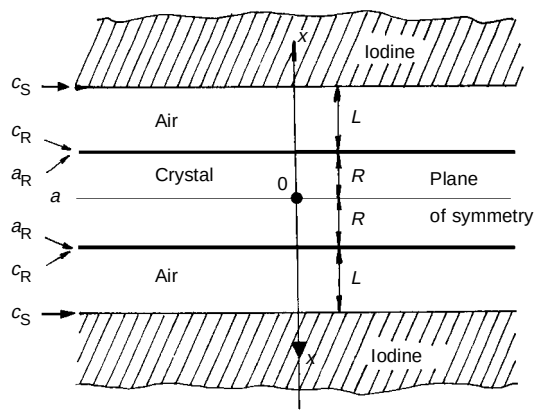

FIG. 11
Schematic representation of Silicalite-1 crystal and iodine particles configuration during colouring procedure from vapour phase

The mathematical formulation of the conditions *1* to *6* is as follows:

From mass conservation and conditions *1*, *2* it follows, that the mass balance equation describing the sorption kinetics of iodine in the crystal can be expressed as

$$R \frac{\mathrm{d}\bar{a}}{\mathrm{d}t} = R \frac{\mathrm{d}a_R}{\mathrm{d}t} = i_R \ , \qquad (A1)$$

where i_R is the mass flow density of iodine at the crystal surface pointing from the gas phase into the crystal bulk.

Further on, from assumption *2* it follows, that the mass balance of the iodine in the gas phase in a layer of the thickness dx located at x takes the form

$$\frac{\partial c}{\partial t} = D_{\mathrm{I_2N_2}} \frac{\partial^2 c}{\partial x^2} \ , \quad \text{for } R < x < R + L \ . \qquad (A2)$$

The boundary conditions to solve Eq. (*A2*) are:

$$c = c_R(t) \quad \text{for } x = R \text{ and}$$

$$c = c_\mathrm{s} \quad \text{for } x = R + L \ . \qquad (A3)$$

Assumption *3* implies the following initial conditions for the problem solved:

$$c = 0 \quad \text{for } x \in \langle R, R + L \rangle \text{ and } t \le 0 \quad \text{and}$$

$$\bar{a} = a_R = 0 \quad \text{for } t \le 0 \ . \qquad (A4)$$

Matching condition at the interface $x = R + L$ is given by the continuity of the mass flow at this interface:

$$i_R = D_{\mathrm{I_2N_2}} \left(\frac{\partial c}{\partial x} \right)_{x=R} \ . \qquad (A5)$$

From assumption *5* it follows that the equilibrium condition at $x = R$ reads as:

$$a_R = \frac{a_\infty B c_R}{1 + B c_R} \ . \qquad (A6)$$

To describe adsorption equilibrium in the system, one makes the following substitution in Eq. (*A6*): $c_R \rightarrow c_s$ and $a_R \rightarrow a_s$, leading to

$$a_s = \frac{a_\infty B c_s}{1 + B c_s} \quad . \tag{A7}$$

Assumption *4* implies, that at $t > 0$ one can practically set $\partial c/\partial t = 0$ in Eq. (*A2*).

Solution of the Model

Integration of equation $d^2c/dx^2 = 0$ together with boundary conditions (*A3*) gives, after combination with Eqs (*A1*) and (*A5*), the kinetic equation:

$$R \frac{d\bar{a}}{dt} = D_{I_2N_2} \frac{c_s - c_R}{L} \quad . \tag{A8}$$

From Eqs (*A6*) and (*A7*) follows:

$$c_R = \frac{a_R}{B (a_\infty - a_R)} = \frac{\bar{a}}{B (a_\infty - \bar{a})} \quad , \tag{A9}$$

and

$$c_s = \frac{a_s}{B (a_\infty - a_s)} \tag{A10}$$

with

$$B = \frac{a_s}{c_s(a_\infty - a_s)} = \frac{S}{(a_\infty - a_s)} \quad , \tag{A11}$$

where $S = a_s/c_s$ represents the slope of the secant of the adsorption isotherm. Substituting Eqs (*A9*)–(*A11*) into (*A8*) one obtains the kinetic equation in the form:

$$\frac{d\bar{a}}{dt} = \frac{D_{I_2N_2}}{RLS} \frac{a_\infty}{(a_\infty - \bar{a})} (a_s - \bar{a}) \quad . \tag{A12}$$

Introducing the dimensionless quantities γ, Θ and u defined by Eqs (*2*)–(*4*) into Eq. (*A12*) one obtains the equation of sorption kinetics in the form

$$\frac{d\gamma}{du} = \frac{1-\gamma}{1-\Theta\gamma} \quad . \qquad (A13)$$

Equation (*A13*) can be integrated *via* separation of variables. Using the initial condition $\gamma = 0$ for $u = 0$, which follows from Eq. (*A4*), the integration results in Eq. (*1*). For $\Theta = 1$, Eq. (*A13*) has a singular point at $u = 1$, $\gamma = 1$ because both the numerator and the denominator on the right hand side of Eq. (*A13*) become equal zero at that point. On the other hand, γ cannot exceed the value $\gamma = 1$. Thus, for physical reasons, the derivative of the kinetic curve becomes discontinuous at the singular point, *i.e.*,

$$\frac{d\gamma}{du} = 1 \quad \text{for } u < 1 \quad \text{and} \quad \frac{d\gamma}{du} = 0 \quad \text{for } u > 1 \quad . \qquad (A14)$$

SYMBOLS

$\bar{a}$	adsorbed amount averaged over volume of the sorbent, mol cm^{-3}
a_R	adsorbed amount of iodine at $x = R$, mol cm^{-3}
a_s	equilibrium adsorbed amount of iodine related to the volume of zeolite crystal, mol cm^{-3}
a_∞	limiting adsorbed amount of iodine related to the volume of zeolite crystal, mol cm^{-3}
B	constant in the Langmuir adsorption isotherm, mol^{-1} cm^3
c	actual concentration of iodine in the vapour phase, mol cm^{-3}
c_R	concentration of iodine in the vapour phase at $x = R$, mol cm^{-3}
c_s	vapour phase concentration of iodine at iodine source (under sorption equilibrium, c_s and a_s are related to each other by sorption isotherm), mol cm^{-3}
$D_{I_2N_2}$	diffusion coefficient for the binary iodine–nitrogen gas mixture, cm^2 s^{-1}
i_R	mass flow density at the crystal surface, mol cm^{-2} s^{-1}
L	distance between the iodine particle and the surface of zeolite crystal, cm
L_i	characteristic dimension of crystal along the crystallographic axis i (i = ***a***, ***b***, ***c***), cm
p	vapour pressure of iodine, Pa
p_s	saturated vapour pressure of iodine at the temperature of sorption, Pa
R	$R = 0.5L_a = 0.5L_b$, cm
S	slope of the secant of sorption isotherm between $c = 0$ and $c = c_s$
t	time, s
u	dimensionless time parameter defined by Eq. (*4*)
x	space coordinate measured from the plane of symmetry of crystal oriented along the outward normal of the surface, cm
γ	relative molecular uptake defined as amount of substance of iodine sorbed in the crystal during time t measured from the beginning of the experiment related to the corresponding equilibrium adsorbed amount, Eq. (*2*)
Θ	loading of crystal by iodine defined by Eq. (*3*)
τ_j	contact time of crystals with the respective fluid (j = v, m, s stands for iodine vapour, saturated solution of iodine in organic solvent, organic solvent, respectively), s
Superscript	
∞	denotes contact time necessary to reach the maximum colouring intensity or the limiting colouring pattern

This work was financially supported by the Grant Agency of the Czech Republic, as the project of the Grant Agency of the Czech Republic No. 203/96/0210 and in a part by the Polish Commitee for Scientific Research (KBN). The authors are indebted to Dr H. G. Karge from Fritz Haber Institute of the Max Planck Society, Berlin for valuable discussion. The authors also wish to thank to Mrs J. Kudova for technical assistance.

REFERENCES

1. Karger J., Ruthven D. M.: *Diffusion in Zeolites*, Chapters 5–7. Wiley, New York 1991.
2. Karger J., Pfeifer H.: *Zeolites* **1987**, *7*, 90.
3. Karger J.: *AIChE J*. **1982**, *28*, 417.
4. Forster C., Karger J., Pfeifer H., Riekert L., Bulow M., Zikanova A.: *J. Chem. Soc., Faraday Trans. 1* **1990**, *86*, 881.
5. Karge H. G., Niessen W.: *Catal. Today* **1991**, *8*, 451.
6. Niessen W., Karge H. G.: *Microporous Mater*. **1993**, *1*, 1.
7. Karge H. G. in: *Introduction to Zeolite Science and Practice* (H. van Bekkum, E. M. Flanigen and J. C. Jansen, Eds), p. 531. Elsevier, Amsterdam 1991.
8. Zikanova A., Derewinski M.: *Zeolites* **1995**, *15*, 148.
9. Micke A., Bulow M., Kocirik M., Struve P.: *J. Phys. Chem*. **1994**, *98*, 12337.
10. Shen D., Rees L. V. C.: *J. Chem. Soc., Faraday Trans*. **1993**, *89*, 1063.
11. Rees L. V. C., Shen D.: *Gas Sep. Purif*. **1993**, *7*, 83.
12. Eic M., Ruthven D. M.: *Zeolites* **1988**, *8*, 40.
13. Micke A., Kocirik M., Bulow M.: *Ber. Bunsen-Ges. Phys. Chem*. **1994**, *98*, 242.
14. Hayhurst D. T., Paravar A. R.: *Zeolites* **1988**, *8*, 27.
15. Geus E. R., van Bekkum H., Bakker W. J. W., Moulijn J. A.: *Microporous Mater*. **1993**, *1*, 131.
16. Caro J., Noack M., Richter-Mendau J., Marlow F., Petersohn D., Griepentrog M., Kornatowski J.: *J. Phys. Chem*. **1993**, *97*, 13685.
17. Micke A., Bulow M., Kocirik M.: *J. Phys. Chem*. **1994**, *98*, 924.
18. Geus E. R., Jansen J. C., van Bekkum H.: *Zeolites* **1994**, *14*, 82.
19. Weidenthaler C., Fischer R. X., Shannon R. D., Medenbach O.: *J. Phys. Chem*. **1994**, *98*, 12687.
20. Price D. G., Pluth J. J., Smith J. V., Bennet J. M., Patton R. L.: *J. Am. Chem. Soc*. **1982**, *104*, 5971.
21. Hay D. G., Jaeger H., Wilshier K. G.: *Zeolites* **1990**, *10*, 571.
22. Reck G., Marlow F., Kornatowski J., Hill W., Caro J.: *J. Phys. Chem*. **1996**, *100*, 1698.
23. Tiselius A.: *Z. Phys. Chem., A* **1934**, *169*, 425.
24. Tiselius A.: *Z. Phys. Chem., A* **1935**, *175*, 401.
25. Karger J., Danz R., Caro J.: *Feingeratetechnik* **1978**, *27*, 539.
26. Kornatowski J.: *Zeolites* **1988**, *8*, 77.
27. Reid R. C., Sherwood T. K.: *The Properties of Gases and Liquids*. McGraw–Hill, New York 1966.
28. Karger J., Zikanova A., Kocirik M.: *Z. Phys. Chem. (Leipzig)* **1984**, *265*, 587.
29. Le Claire A. D. in: *Treatise on Solid State Chemistry* (N. B. Hannay, Ed.) Vol. 4, p. 16. Plenum Press, New York 1976.